CSIRO PUBLISHING

International Journal of Wildland Fire **2015**, *24*, 276–285
http://dx.doi.org/10.1071/WF13071

Fire emission uncertainties and their effect on smoke dispersion predictions: a case study at Eglin Air Force Base, Florida, USA

Aika Y. Davis[A], *Roger Ottmar*[B], *Yongqiang Liu*[C], *Scott Goodrick*[C], *Gary Achtemeier*[C], *Brian Gullett*[D], *Johanna Aurell*[D], *William Stevens*[E], *Roby Greenwald*[F], *Yongtao Hu*[A], *Armistead Russell*[A], *J. Kevin Hiers*[G] and *M. Talat Odman*[A,H]

[A]School of Civil and Environmental Engineering, Georgia Institute of Technology, 790 Atlantic Drive, Atlanta, GA 30332, USA.
[B]USDA Forest Service, Pacific Northwest Research Station, Pacific Wildland Fire Sciences Laboratory, 400 N 34th Street, Seattle, WA 98103, USA.
[C]USDA Forest Service, Southern Research Station, Forestry Sciences Laboratory, 320 Green Street, Athens, GA 30602, USA.
[D]US Environmental Protection Agency Office of Research and Development, National Risk Management Research Laboratory, 109 T. W. Alexander Drive, Research Triangle Park, NC 27711, USA.
[E]Campus Box 2056, Kentucky Christian University, 100 Academic Parkway, Grayson, KY 41143, USA.
[F]Rollins School of Public Health, Emory University, 1518 Clifton Road, Atlanta, GA 30322, USA.
[G]Environmental Stewardship and Sustainability, University of the South, 735 University Avenue, Sewanee, TN 37383, USA.
[H]Corresponding author. Email: talat.odman@ce.gatech.edu

Abstract. Prescribed burning is practiced to benefit ecosystems but the resulting emissions can adversely affect air quality. A better understanding of the uncertainties in emission estimates and how these uncertainties affect smoke predictions is critical for model-based decision making. This study examined uncertainties associated with estimating fire emissions and how they affected smoke concentrations downwind from a prescribed burn that was conducted at Eglin Air Force Base in Florida, US. Estimated variables used in the modelled emission calculation were compared with field measurements. Fuel loadings, fuel consumption and emission factors were simulated using Photo Series, Consume, and previously published values. A plume dispersion model was used to study the effect of uncertainty in emissions on ground concentration prediction. The fire emission models predicted fuel loading, fuel consumption and emission factor within 15% of measurements. Approximately 18% uncertainty in field measurements of $PM_{2.5}$ emissions and 36% uncertainty attributed to variability in emission estimating models resulted respectively in 20% and 42% ground level $PM_{2.5}$ concentration uncertainties in dispersion modelling using Daysmoke. Uncertainty in input emissions influences the concentrations predicted by the smoke dispersion model to the same degree as does the model's inherent uncertainty due to turbulence.

Received 25 May 2013, accepted 23 October 2014, published online 3 February 2015

Introduction

Prescribed burning is practiced throughout the world for ecological and safety reasons, and it is mostly practiced in temperate forests (Seiler and Crutzen 1980) including in Australia (Fernandes *et al.* 2013), Europe (Montiel and Kraus 2010) and the south-eastern US (Tian *et al.* 2009). Prescribed burning is used to prepare the ground for tree seeding and planting; control disease and tree competition; manage understory debris and perpetuate fire-dependent plant species. Prescribed burning can also improve wildlife habitat (e.g. for threatened animal species) and reduce wildfire risk. However, prescribed burning produces smoke and releases gases that may reduce air quality in local urban areas (Hu *et al.* 2008; Liu *et al.* 2009). The smoke can also contribute to regional haze that reduces visibility in scenic areas and along major traffic corridors (Achtemeier 2008). The US Environmental Protection

Agency (EPA) 2011 National Emission Inventory (US EPA 2013) reported that 15% (8.4×10^8 kg) of $PM_{2.5}$ (i.e. particulate matter less than 2.5 μm in aerodynamic diameter) emissions in the US are attributable to prescribed burning, and 27% of $PM_{2.5}$ emissions from prescribed burning originate from the south-eastern US. Prescribed burning emissions remain one of the most prominent sources of $PM_{2.5}$ in the south-eastern US, and will become an increasing fraction as other sources are controlled.

Responsible practice of prescribed burning entails accurate predictions of air quality effects to mitigate the potential to adversely affect air quality in heavily populated regions. Several modelling tools are available for use in prescribed burning management (Andrews *et al.* 2003; Anderson *et al.* 2004; Prichard *et al.* 2007; Larkin *et al.* 2009; Achtemeier *et al.* 2011; Ottmar 2014; Weise and Wright 2014). The models are used to estimate fuel consumption, smoke emissions, plume transport and dispersion, and whether the pollutants would influence air quality in urban areas. Whether simple or complex, all models and their predictions are subject to uncertainty.

Several field and modelling studies have been conducted to better quantify prescribed burning emissions and associated uncertainties: French *et al.* (2004), Wiedinmyer *et al.* (2006), Tian *et al.* (2009) and Urbanski *et al.* (2011). However, few studies have examined the effect of emission uncertainties on local air quality predictions. In this study, data were collected from a comprehensive field campaign called the Prescribed Fire Combustion and Atmospheric Dynamics Research Experiment (Rx-CADRE). Rx-CADRE was conducted at Eglin Air Force Base (AFB) near Niceville, Florida, US (Fig. 1). It provided a unique opportunity to evaluate uncertainties in emissions derived from measurements as well as emissions predicted by fire models. The magnitude of the effect on smoke dispersion predictions from emission uncertainty was evaluated through a plume dispersion model. With a better understanding of uncertainties associated with estimated emissions and downwind concentrations, land managers should be able to better assess whether a burn would lead to violation of air quality regulations such as the US National Ambient Air Quality Standards (NAAQS).

Site and burn description

The Rx-CADRE prescribed burn monitored for this study was unit 608A, a reasonably flat unit, located at 30°38′39″N, 86°16′37″W in Eglin AFB (Fig. 1). The 831-ha (2054-acre) unit was burned on 8 February 2011. Clear skies were observed with winds shifting from north to north-easterly during the burn. The fuel bed was classified as managed long leaf pine (*Pinus palustris*) and turkey oak (*Quercus laevis*) forest with an understorey of little bluestem (*Schizachyrium scoparium*), palmetto (*Serenoa repens*) and grass (*Andropogon virginicus*). Long leaf pine litter was the main fuel that carried the fire. A helicopter started a backing fire at 1159 hours Central Standard Time (CST) and finished the first part of the ignition at 1251 hours CST. In the second part, a head fire was started at 1323 hours CST and completed at 1356 hours CST. The fuels continued to be consumed until 1420 hours CST. A tethered aerostat – a balloon with instruments restrained by cables attached to a vehicle – was launched to obtain measurements required for emission calculations near the burn site (Fig. 1). The ground level concentration of $PM_{2.5}$ was measured at two sites: a stationary site at 4.0 km downwind, and Mobile 2 site at 9.2 km downwind (Fig. 1). Initially these sites were roughly under the centreline of the plume, but when the wind shifted, the sites were off centred.

Materials and methods

Prescribed burning emissions, E, for specific fuel types were calculated by multiplying the fuel loading consumed (FC, mass of burned vegetation per unit area) by an emission factor (EF, mass of compound emitted per mass of burned vegetation) and the total area burned, A (Seiler and Crutzen 1980).

$$E = \mathrm{FC} \times \mathrm{EF} \times \mathrm{A} \quad (1)$$

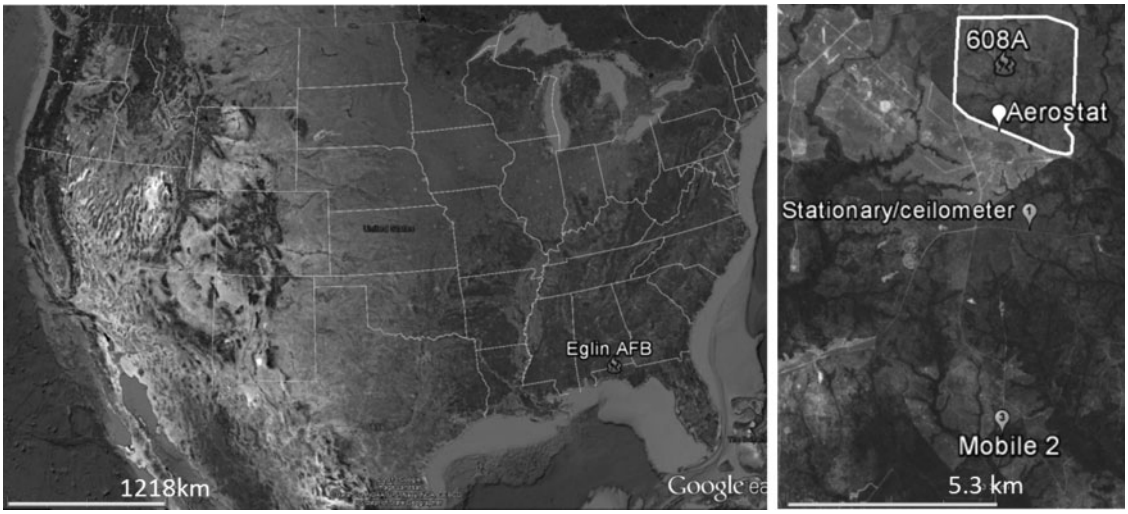

Fig. 1. Location of Eglin AFB in Florida, US (left) and a map of the burn site, showing Unit 608A bordered in white, the site of the aerostat and sonic anemometer at 1.4 km away from fire centre (white balloon), the stationary and ceilometer site 4.0 km away (balloon #1), and Mobile 2 site 9.2 km away (balloon #3), shown on Google Earth (GoogleEarth7.1 2013).

Fuel loading was studied first, followed by fuel consumption, emission factor, emissions and plume dispersion (Fig. 2). On-site measurements and model predictions were compared for each variable studied. Measurement procedures and modelling methods are described in the following sections.

Fuel loading

Fuel loading is the total amount of vegetation that is on the site (mass per unit area). For both pre- and post-fire fuel loading measurements, standard ground-based inventory techniques (Brown 1974) were used. There were three sampling locations, each representing one of the three distinctive vegetation types in unit 608A. Twenty destructive clip plots (1 m^2 each) were collected at each sampling location. All biomass was sorted by fuel bed components including litter (all non-decomposed dead plant material including needles, leaves, etc.), duff (fermentation and humus layers) and understorey vegetation biomass including herbaceous vegetation (grass and herbs), woody vegetation (shrubs and seedlings), palmetto, and 1-h, 10-h and 100-h time lag dead woody fuels (representing woody fuel diameters of 0–0.60 cm, 0.61–2.5 cm and 2.6–7.6 cm). The fuel material was oven dried at 70°C, then weighed to determine the dry fuel mass using area weighted averages of three fuel loadings (Table 1). As there were very few logs and little duff, those two fuel bed components were not measured.

The fuel loading before the burn was predicted by the Stereo Fuels Photo Series for Quantifying Fuels, Volume VIa (Ottmar *et al.* 2003). The fuels were identified closely to Sand hill (SH) 10 within the series with its cover type defined as Longleaf Pine-Scrub Oak (Society of American Foresters (SAF) 071). Very little duff was observed on site; therefore duff was assumed to be negligible and was not considered in fuel loading estimation. Listed values of fuel loadings for woody and surface material were compared with field measurements (Table 1). The summation over all fuel loadings for each fuel type is the total fuel loading.

Fuel consumption

Fuel consumption is the amount of vegetation that burned during the fire (mass per unit area). The measured fuel consumption was determined by taking the difference between measured pre- and post-burn fuel loadings. The 20 post-burn destructive clip plots were offset from the pre-burn clipped plots to obtain post-burn fuel loading. The different fuel species remaining after the burn were separated into four different fuel bed categories: shrubs (i.e. living and dead palmetto, woody shrub, yucca), grass (i.e. wiregrass, other grass, live and dead forbs), woody debris of all sizes smaller than 7.6 cm in diameter and litter. The averages of each fuel bed category are presented in Table 1.

Consume 3.0 (Prichard *et al.* 2007) was used to predict how much of the fuel loading estimated from the Photo Series would be consumed by the fire. Consume takes in fuel characteristics, lighting patterns, fuel conditions and meteorological attributes, and outputs fuel consumption by fuel bed categories. The following decisions were taken when running the model: (1) the crown consumption was set to zero because the objective of this prescribed fire was to burn in such a way that minimised crown consumption; (2) an ocular estimation rather than a true inventory was used because of limited inventory time and because 80% of the shrubs were detected to be alive and (3) the measured values for the depth (2.5 cm, or 1 inch) and the fuel coverage of litter (70% coverage of the ground) were also used.

Fuel moisture is a significant factor in combustion efficiency (Grandesso *et al.* 2011). Therefore, the measured fuel moisture values were used in Consume to minimise the effect of fuel moisture uncertainty on the consumption calculations. Fuel moisture values were determined by collecting samples of fuels immediately before the burn and weighing the samples.

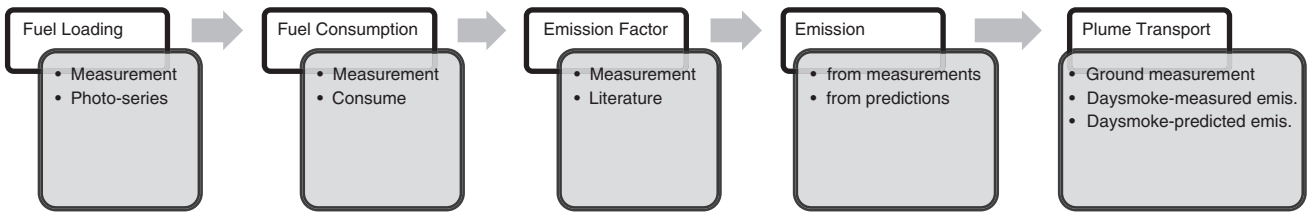

Fig. 2. Framework used to predict fire emissions and plume transport. Calculated variables are shown in the top white boxes and different ways of obtaining the variable are listed under each variable.

Table 1. Photo-series-estimated *v.* measured fuel loadings and consumptions modelled by Consume *v.* measured consumptions by fuel type for Unit 608A at Eglin Air Force Base on 8 February 2011

Woody fuel debris consumptions are summed to one number; 60 samples were averaged

		Woody fuels			Shrub	Non-woody	Litter	Total
		1-h	10-h	100-h				
Fuel loading (kg m^{-2})	Field measurement	0.01	0.05	0.11	0.02	0.08	0.33	0.59
	Photo series	0.02	0.07	0.09	0.01	0.03	0.44	0.66
Consumption (kg m^{-2})	Field measurement		0.10		0.01	0.07	0.30	0.49
	Photo/Consume		0.09		0.00	0.03	0.44	0.56

Table 2. Measured fuel loading, fuel consumption and $PM_{2.5}$ emission factor *v.* Photo-series-estimated fuel loading, fuel consumption modelled by Consume, and mean of published emission factors for Eglin Air Force Base

	Fuel loading (kg m^{-2})	Fuel consumption (kg m^{-2})	$PM_{2.5}$ emission factor (g kg^{-1})	$PM_{2.5}$ emissions (kg)
Measured	0.59 ± 0.06	0.49 ± 0.06	14 ± 1.9	5.69×10^4
Modelled	0.66	0.56	13	6.08×10^4
Difference	11%	15%	−7%	7%

The same samples were later dried for 48 h at a minimum of 70°C and reweighed to obtain the percentage fuel moisture content for each fuel bed category. The total mass of fuel consumed per unit area was calculated by summing the fuel consumptions for each fuel bed category.

Emission factor

The $PM_{2.5}$ emission factor specific to this case study was derived from the filter sample collected by the aerostat located within 200 m of the burn site. The average $PM_{2.5}$ concentration derived from the filter sample was converted to an emission factor using the carbon mass balance approach (Laursen *et al.* 1992). The carbon mass balance method assumes that all the carbon released by combustion was measured. The average $PM_{2.5}$ concentration divided by the sum of averages of measured carbon species and multiplied by carbon fraction in the biomass is the emission factor. Fifty percent of the biomass was assumed to be carbon. Although the majority of carbon emitted is CO or CO_2, not all carbon species from combustion can be measured. Therefore, the $PM_{2.5}$ emission factor derived from the carbon mass method tends to be slightly overestimated. Details on the aerostat's measurements and emission factor calculation can be found in Aurell and Gullett (2013). The product of measured fuel consumption, emission factor and the area of the burn is referenced as the total measured emissions, and this is listed in Table 2. The area of the burn was assumed to be equal to the area of unit 608A.

In emission modelling, emission factors are typically obtained from the literature. Emission factors applicable to biomass at Eglin AFB were collected from various sources. In the US EPA AP-42 database (US EPA 1995), the $PM_{2.5}$ emission factor for conifer long needle biomass (13 g kg^{-1}) was assumed to be the most appropriate for this study. Urbanski *et al.* (2008) listed $PM_{2.5}$ emission factors from various burns conducted throughout the US (6.9 g kg^{-1}) and from previous measurements specific to Eglin AFB (11.9 g kg^{-1}). Aurell and Gullett (2013) listed $PM_{2.5}$ emission factors obtained from another Rx-CADRE burn using filter measurements (13 g kg^{-1}) and simulated burns at an open burn test facility using fuels collected at Eglin (12, 15 and 19 g kg^{-1}). The mean and standard deviation of the mentioned $PM_{2.5}$ emission factors were 13 and 3.4 g kg^{-1}. The mean value was used as the modelled emission factor. The total modelled emissions were calculated by taking the product of the modelled fuel consumption with this emission factor and the area of the burn.

Plume dispersion

Lagrangian stochastic models are often applied to follow tracer particles in turbulent flow, and this type of model is especially suitable for quantifying how emissions from a particular source influence air quality (Wilson and Sawford 1996). This prescribed burn was simulated using Daysmoke, an empirical–stochastic fire plume model developed specifically for prescribed burns in the south-eastern US (Achtemeier *et al.* 2011). Daysmoke requires emission rates, updraft core numbers (the number of discernable, organised, rising plumes in a burn), updraft core vertical velocities, maximum initial updraft core diameters and vertical profiles of meteorological data as inputs for every 12 min (Achtemeier *et al.* 2011; Achtemeier *et al.* 2012). The ambient vertical temperature profile was used in the calculations that determine plume stability and plume height.

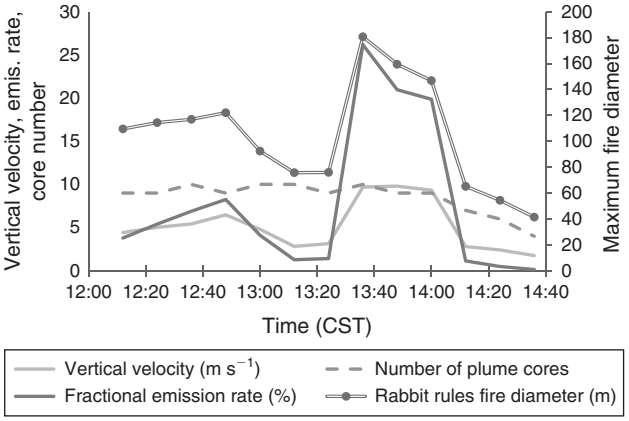

Fig. 3. Time-dependent updraft core vertical velocity, updraft core number, maximum initial updraft core diameter and fractional emission rates produced by Rabbit Rules (Achtemeier *et al.* 2012).

Time profile of heat release and relative emission rates

Location and number of updraft cores, updraft core vertical velocities, maximum initial updraft core diameters, fractional emission rates and the percentage of total emission per unit time were all obtained from a cellular automata fire spread model called Rabbit Rules (Achtemeier *et al.* 2012). Twelve-min averages of these variables (Fig. 3) were used. In all Daysmoke simulations, the updraft core numbers and the updraft core vertical velocities from Rabbit Rules were kept the same. Emission rates were derived by multiplying the fractional emission rates with the total measured or modelled emissions (Fig. 4).

The Daysmoke simulation using emissions calculated from the field measurements used the maximum initial updraft core diameters directly from Rabbit Rules. To obtain the maximum initial updraft core diameter (*Fdia*) commensurate with

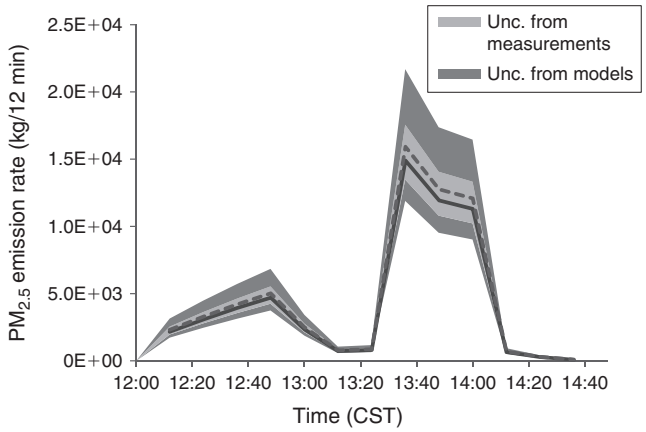

Fig. 4. Time-dependent emission rates included in Daysmoke simulations for the 608A burn on 8 February 2011. The lines show the measurement-derived emissions (solid) and modelled emissions (dotted). Shaded areas are the uncertainty ranges due to measurement uncertainty (light grey) and due to modelled emission variability (dark grey).

predicted emissions from the modelled case, the initial updraft core diameter from Rabbit Rules was adjusted following its relationship with heat release (Q), $Q \propto Fdia^2$, from Mercer and Weber (2001). The hourly heat release rate was obtained from the Fire Emission Production Simulator (FEPS) (Anderson *et al.* 2004). FEPS requires information such as fuel loading, fuel moisture, total consumption per acre, area burned per hour, and start and end times of ignition. FEPS was applied twice, once with measured fuel consumptions and the other time with estimated fuel consumptions from Consume 3.0. As a helicopter ignited the burn and there was very little duff or large woody fuels, the fire burned efficiently, leading to an estimated 95% fuel bed involvement in the flaming combustion stage and the remaining 5% in the long-term smouldering stage.

Meteorology

Other sources of uncertainty in smoke dispersion simulations include model formulation, atmospheric stability, wind speed and most importantly, wind direction (Jain *et al.* 2007; Garcia-Menendez *et al.* 2013). As this study focussed on emission uncertainty, meteorological prediction uncertainties were minimised by modifying modelled wind profiles to best match the observations (details in Supplementary Material available online only at http://www.publish.csiro.au/?act=view_file&file_id=WF13071_AC.pdf). The Weather Research and Forecasting (WRF) modelling system (Skamarock *et al.* 2008; Skamarock and Klemp 2008) was used for simulating local meteorology. Corrections were made to the simulated meteorological vertical profiles taken at the centre of the burn site. Real-time wind measurements at different altitudes ranging from 2–280 m were taken at three different locations: one by the aerostat and two others on the ground. The WRF wind speeds were adjusted to fit the logarithmic wind profile (Holton 2004) in a least-squares sense for these three measurements. The WRF wind directions were shifted to fit the simplified Ekman spiral profile (Holton 2004), also in a least-squared sense for three wind direction measurements. WRF underestimated the observed rotation in wind direction by altitude; therefore, the WRF-simulated winds were rotated up to 35° clockwise over the 3-h burn period. Vertical profiles of the adjusted wind speed and wind direction, and unadjusted temperature and relative humidity from WRF were input to Daysmoke.

Plume height

Daysmoke assigns a smoke parcel to every 1 kg of $PM_{2.5}$ emitted and tracks the trajectory of those parcels in a Lagrangian stochastic framework (Achtemeier *et al.* 2011). The coordinates of the smoke parcels were used to predict the plume height and the ground concentration. To characterise the random variability in Daysmoke, the model was run 40 times for each emissions case: one with emission rates derived from the measurements and fire diameter directly from Rabbit Rules, and the other with modelled emission rates and modified fire diameter using the relationship with heat release. The remaining required variables were kept constant for all Daysmoke simulations. From the 40 Daysmoke outputs, the mean and the standard deviation of the plume heights and the downwind concentrations were calculated at 10-min intervals.

Simulated plume heights were evaluated with plume height measurements from Vaisala CL31 backscatter ceilometer designed around laser LIDAR technology (Liu *et al.* 2013). The ceilometer emits short, powerful laser pulses at a wavelength of 0.9 μm in a vertical or slant direction. The backscattered light from aerosols found in the smoke plume, which is dominated by particles with a diameter of 1 μm and smaller (Reid *et al.* 2005), is measured as the LIDAR scans the sky. The ceilometer has a range of 7.5 km at a resolution of 20 m, with a detection frequency as high as 2 s. This ceilometer was located 4 km away from the burn (Fig. 1). The Daysmoke plume heights were calculated as the average height of the simulated smoke parcels near the ceilometer. Ten-minute averages of Daysmoke-simulated and measured plume heights were compared.

Ground concentration

Daysmoke's performance was evaluated using measured ground level $PM_{2.5}$ concentrations at 4.0 and 9.2 km downwind from the burn site. Two continuous sampling instruments, a Tapered Element Oscillating Microbalance or TEOM (Thermo Scientific, Waltham, MA) and an AeroTrak handheld particle counter Model 9306 (TSI Inc., Shoreview, MN), both sampling at 10-s time step, were used. AeroTrak was available at both measurement sites and TEOM was used at the closer site to verify the AeroTrak measurements as well as to calculate the measurement uncertainty associated with ground concentrations. The average concentrations of 40 Daysmoke runs at the two study sites were compared with the averages of AeroTrak measurements at every 10 min.

Error analysis

Two measures of model performance were calculated; the root mean squared error (RMSE) and the mean fractional error (MFE). RMSE aggregates the magnitudes of the errors in predictions and is expressed as:

$$RMSE = \sqrt{\frac{1}{n}\sum_{i=1}^{n}(P_i - O_i)^2} \qquad (2)$$

where O_i is the ith measured ground concentration out of n concentration measurements, and P_i is the ground concentration simulated by Daysmoke. MFE is often used in concentration comparisons because it has the advantage of equally weighting the biases for small and large predictions or observations (Boylan and Russell 2006). Using the same notation as RMSE, MFE is expressed as:

$$MFE = \frac{2}{n}\sum_{i=1}^{n}\frac{|P_i - O_i|}{(P_i + O_i)} \quad (3)$$

The modelled emissions and the measurement-derived emissions were also compared with these two metrics. Increases in RMSE and MFE due to input emission uncertainties were also studied.

Uncertainty

Measurement uncertainties in fuel loading, fuel consumption, δFC, and emission factor, δEF, were estimated (Table 2) and propagated to estimate the total emission uncertainty, δE:

$$\frac{\delta E}{E_{meas.}} = \sqrt{\left(\frac{\delta FC}{FC_{meas.}}\right)^2 + \left(\frac{\delta EF}{EF_{meas.}}\right)^2} \quad (4)$$

The upper and lower bounds of total emissions, $E_{meas.} \pm \delta E$, were converted into emission rates using the fractional emission rates as described previously. The area between these two bounds is coloured in lighter grey in Fig. 4. The two sets of emission rates were input into Daysmoke and were simulated 40 times each. The 10-min averages of $PM_{2.5}$ ground concentrations at the two measurement sites as well as across the plume at 9.2 km downwind were used as the basis to study the effect of input emissions uncertainty on ground concentration uncertainty. For the analysis across the plume, the concentrations were extracted from 10 equally spaced points within the plume width.

The differences of modelled values from measured values, $\Delta x = x_{modelled} - x_{measured}$, were also studied. As there were multiple emission factors to choose from, we defined the difference of 'modelled' emission factor as:

$$\Delta EF = |EF_{modeled} + \sigma_{EF} - EF_{measured}|$$

for the upper bound and

$$\Delta EF = |EF_{modeled} - \sigma_{EF} - EF_{measured}| \quad (5)$$

for the lower bound.

The difference in total emissions, ΔE, is defined as:

$$\frac{\Delta E}{E_{modeled}} = \sqrt{\left(\frac{\Delta FC}{FC_{modeled}}\right)^2 + \left(\frac{\Delta EF}{EF_{modeled}}\right)^2}. \quad (6)$$

The upper and lower deviation bounds of total emission were also converted to emission rates (shaded in darker grey in Fig. 4), and simulated in Daysmoke. Similarly, the 10-min averages of $PM_{2.5}$ ground concentrations at the three studied areas were extracted.

Results and discussion

Model evaluation

Plume heights estimated by Daysmoke were in agreement with measured plume height from the ceilometer (Fig. 5). The predicted plume heights using measurement-derived emissions and modelled emissions were consistently within one standard deviation of the measurements. The ceilometer measurements had a large standard deviation because the wind conditions caused the plume to be turbulent, and the plume height to vary frequently over time. Daysmoke did not capture the first sharp increase in the observed plume height at 1230 hours CST but instead simulated a gradual increase over time, similar to the fire diameter predicted by Rabbit Rules (Fig. 3). Daysmoke predicted the second increase in plume height that occurred during the second part of ignition, which was represented in the model by fractional emission rates and fire diameters increasing around 1330 hours CST. The ceilometer measured the average plume height to be 860 m, and Daysmoke's average plume height using measurement-derived emissions was 760 m with MFE of 16%. The average plume height simulated using modelled emissions was 780 m with MFE of 13%, which was closer to the measurements than the case with measurement-derived emissions. Since the modelled fuel consumption was larger than the measured fuel consumption, the plume using the modelled emissions had larger heat release. With more heat released, the plume was more buoyant, leading to a 3% higher plume height than that from measurement-derived emissions.

Before comparing the dispersion model results to measured $PM_{2.5}$ ground concentrations, the uncertainty within the ground measurements was studied. The sets of measurements by AeroTrak and TEOM were compared against each other, and had a correlation, R, of 0.83 (Fig. 6). The correlation between the two AeroTraks was 0.98.

Time series comparison of the two sets of Daysmoke-simulated ground level $PM_{2.5}$ concentrations against the

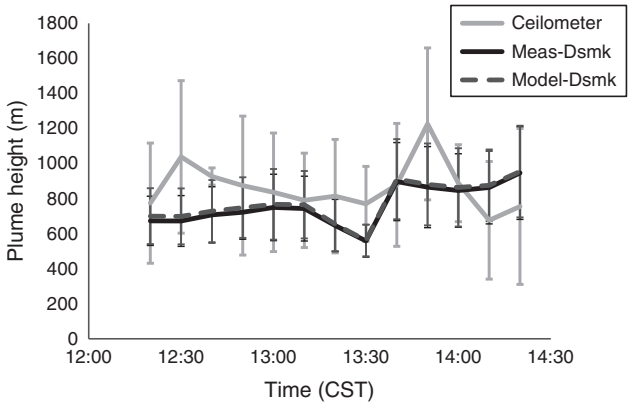

Fig. 5. Ten-minute average plume height comparison between ceilometer measurement (light grey) and Daysmoke-simulated plume heights using emissions calculated from measurements (dark solid line) or modelled emissions (dashed line) at 4.0 km downwind. Error bars represent ceilometer's measurement uncertainty or modelling uncertainty.

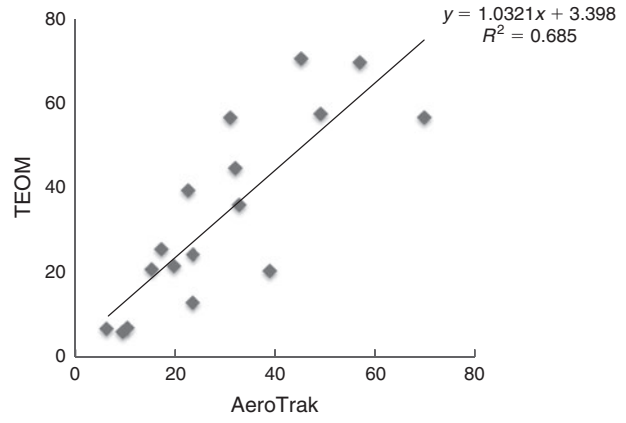

Fig. 6. The 10-min average concentrations (μg m^{-3}) derived from AeroTrak particle counter compared with TEOM measurements

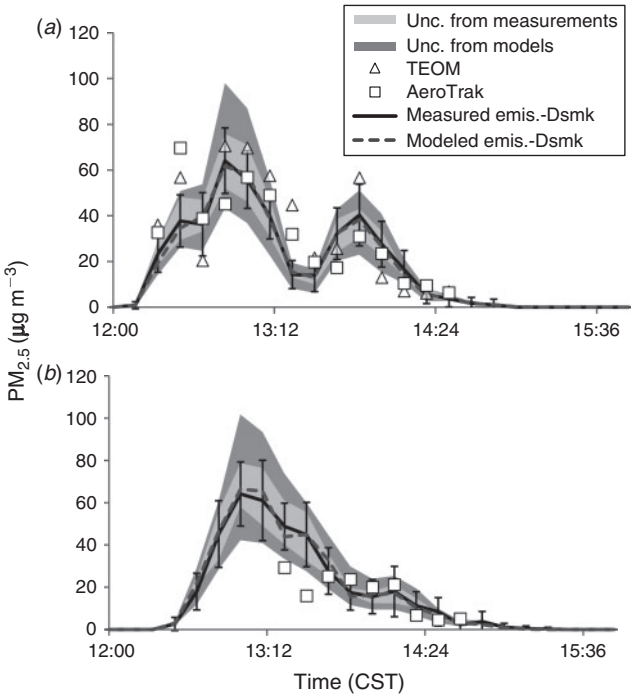

Fig. 7. Comparison of 10-min average ground concentration predictions with measurements at 4.0 km (*a*) and 9.2 km (*b*) away from the burn. The lines show the mean of 40 Daysmoke runs using measurement-derived emissions (solid) and modelled emissions (dotted). Shaded areas are the uncertainty ranges due to the uncertainty in measured emission variables (light grey) and due to modelled emission variability (dark grey). Error bars show the concentration standard deviations from the 40 Daysmoke runs with measurement-derived emissions.

measurements are shown in Fig. 7. The $PM_{2.5}$ concentration measurements taken 4 km downwind showed that the concentration increased from the background level due to the smoke for the first 2 h after ignition. Similar to plume height, the concentration at 4 km away from the fire started increasing at 1330 hours CST. Mobile 2 was busy chasing for the plume at the beginning of the simulation; therefore the measurements were only collected after 1310 hours CST at 9.2 km downwind. As the wind shifted direction, the plume shifted away from the measurement sites. Therefore, the measured $PM_{2.5}$ concentrations at both measurement sites started decreasing after 1400 hours CST. Daysmoke simulations were able to capture this shift due to changing wind direction, and the simulated ground concentrations decreased around the same time as the measurements did. RMSE and MFE of Daysmoke predictions using emissions calculated from the field measurements (labelled as measured emis.-Dsmk) at 4 km downwind against 14 10-min averages of TEOM measurements were 14.5 μg m^{-3} and 45%, and against 14 averages of AeroTrak measurements were 12.8 μg m^{-3} and 37%. The difference in MFE with respect to measurement discrepancy by TEOM and AeroTrak was only 8%. Daysmoke with measurement-derived emissions showed a decrease in $PM_{2.5}$ concentration measured at Mobile 2 site. RMSE and MFE against nine averages of AeroTrak measurements were 12.2 μg m^{-3} and 46%.

Uncertainty analysis

Measured and modelled fuel loadings differed by only 11% (Table 2). Estimating fuel loading and fuel consumption is usually one of the most difficult parts in estimating emissions. However, since the burn unit in this study had a relatively small amount of fuel with very little coarse woody debris and duff, the fuel loading and fuel consumption were estimated with great accuracy (Table 2 and Table 1). For other cases, the uncertainty associated with fuel loading can be much larger (Keane 2012). The greatest difference between modelled and measured variables for the three studied was for fuel consumption (Table 2). The net difference between the modelled and the measured total emissions was 7%. The RMSE and MFE of Daysmoke simulations against the AeroTrak measurements averaged for both measurement sites are shown in Table 3. The modelled emissions case has 7% larger total emissions and 3% higher plume height than the measurement-derived emissions case. The Daysmoke predicted ground level $PM_{2.5}$ concentrations using modelled emissions were closer to the observations with 2% lower MFE than the concentrations predicted using measurement-derived emissions.

Daysmoke's stochastic formulation led to a large variability in simulated ground level concentrations. The bars in Fig. 7 represent the standard deviation of 40 Daysmoke predictions with the same emission inputs at a particular time. The standard deviation represents, in part, the uncertainty inherent to turbulence. Daysmoke's standard deviation at these two sites was usually half of estimated $PM_{2.5}$ concentrations and was as large as 19.0 μg m^{-3} for concentrations ~20 μg m^{-3}. Daysmoke's standard deviation was as large as or even larger than the uncertainties from input emissions (the grey shaded areas in Fig. 7), especially at lower concentrations.

Uncertainty introduced in total $PM_{2.5}$ emissions due to fuel consumption and emission factor measurement uncertainties was 1.02×10^4 kg, or 18% of the total emissions (Table 3). The effect of emission measurement uncertainty in Daysmoke concentration simulation (lighter grey in Fig. 7) is 7.3 μg m^{-3} in the RMSE and 20% in the MFE. Uncertainty in total emissions due

Table 3. Root mean squared error (RMSE) and mean fractional error (MFE) of Daysmoke $PM_{2.5}$ predictions with measurement-based emissions (top row) and model-based emissions (bottom row) against both sets of AeroTrak measurements, total input emission uncertainties and their effect on ground concentration uncertainties

	Error against AeroTrak		Total emission uncertainty	Uncertainty in ground concentration due to emissions uncertainty	
	RMSE (μg m^{-3})	MFE (%)	(kg)	RMSE (μg m^{-3})	MFE (%)
Daysmoke-measured	14.0	44	Standard error 1.02×10^4 (18%)	7.3	20
Daysmoke-modelled	13.0	42	Standard deviation 2.20×10^4 (36%)	14.4	42

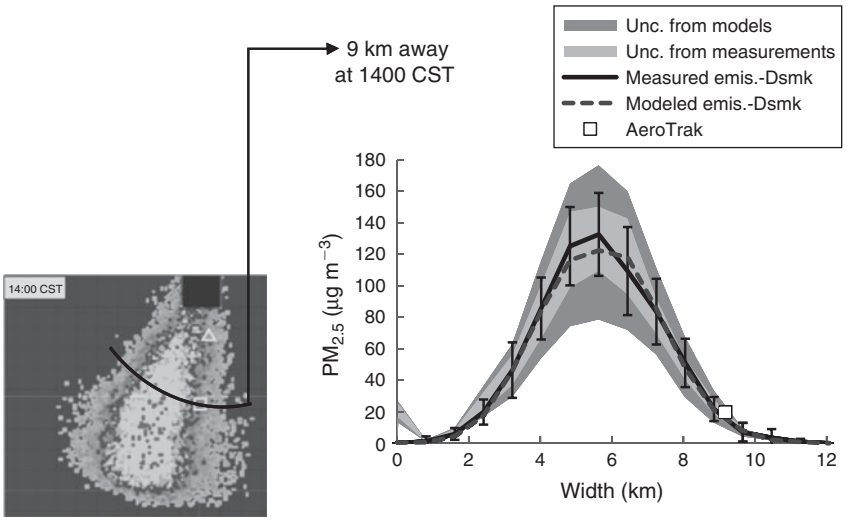

Fig. 8. Bird's eye view from Daysmoke at 1400 hours CST on 8 February 2011 (left) with an arc representing where the cross-sectional analyses were performed. Comparison of 10-min averaged ground concentration predictions with measurements at 1400 hours CST, 9.2 km (right) away from the burn. The lines show the mean of 40 Daysmoke runs using measurement-derived emissions (solid) and modelled emissions (dotted). Shaded areas are the uncertainty ranges due to the uncertainty in measured emission variables (light grey) and due to modelled emission variability (dark grey). Error bars show the concentration standard deviations from the 40 Daysmoke runs with measurement-derived emissions.

to modelling uncertainty was calculated from the differences in modelled and measured values listed in Table 2. The difference between the modelled and the measured values increased from fuel loading to fuel consumption, but decreased for emission factor. The difference in fuel consumption (0.07 kg m^{-2}) and the difference in emission factor (1 g kg^{-1} plus one standard deviation of 3.4 g kg^{-1}) led to 2.20×10^4 kg difference in total emissions (36% of total emissions). The difference in total emissions was larger than the field measurement uncertainty. The emissions modelling variability affected Daysmoke predictions (darker grey in Fig. 7) by RMSE of 14.4 μg m^{-3} and MFE of 42%, which is almost twice as large as the uncertainty introduced by measurements.

It can be seen from the snapshot of the plume at 1400 hours CST (Fig. 8) that the measurements were sometimes taken at the edge of the plume due to the shifting plume. Similar uncertainty analyses were also conducted across the plume for the duration of the burn at 9.2 km downwind. An example analysis at 1400 hours CST is shown in Fig. 8. As expected, the concentration increased towards the centre of the plume. Simulations using modelled emissions led to slightly lower concentrations. Uncertainty in ground concentration introduced from emission measurement uncertainty could be as large as 24.1 μg m^{-3} at the centre of the plume. Uncertainty in ground concentration due to modelled emission variability could be even larger, 48.9 μg m^{-3}. Daysmoke's standard deviation was at times as large as 27.9 μg m^{-3} at the centre of the plume, but was only 26% of predicted concentration at the centre of the plume. Although Daysmoke's standard deviation was larger than the uncertainty in ground concentrations due to measurement and modelling uncertainty in emissions at the edge of the plume, the dispersion model's standard deviation was smaller than the uncertainty from the emissions near the centre of the plume. Therefore, measurement and modelling uncertainties in emissions are just as important as inherent Daysmoke uncertainty due to turbulence.

Conclusion

Uncertainties in fuel loading, fuel consumption, emission factors and their effect on simulated ground concentrations were analysed in the present study. In this case study, the models predicted fuel loading and fuel consumption within 15% of measured values. Although the previously published emission factors applicable for the study area ranged from 6.9 to 19 g kg^{-1}, their mean was only 7% lower than the emission factor measured in our study. The calculated total $PM_{2.5}$ emissions calculated from modelled values differed from the measured emissions values by 7%. Daysmoke results had a large uncertainty due to the meteorological and model-related uncertainties. By adjusting the WRF-simulated wind speed and wind direction with the field-measured values, the errors introduced through meteorological inputs were minimised. The dispersion model's performance was evaluated by comparing plume heights and downwind smoke concentrations against measurements. Simulated plume heights had a slightly low bias compared with the measurements and MFE of 16%. Daysmoke was able to predict the ground concentrations with a RMSE of 14.5 μg m^{-3}.

Variability in modelled emissions was larger than measurement uncertainty. Measurement uncertainties in fuel loading, fuel consumption and emission factor were combined using propagation of error, and resulted in 18% uncertainty in total $PM_{2.5}$ emissions. The differences between the modelled and measured values in fuel loading, fuel consumption and emission factor, and the large variability in modelled emission factors led to a 36% uncertainty in modelled total emissions. Measurement uncertainty in the input emissions led to 20% uncertainty in simulated $PM_{2.5}$ concentrations, and variability in modelled emissions led to 42% concentration uncertainty. Predicted concentrations and emission-related uncertainties increased towards the centre of the plume. This study found that uncertainty derived from input emissions had a greater contribution to the overall uncertainty in concentrations predicted by the smoke dispersion model when compared with the model's inherent uncertainty attributed to the stochastic nature of turbulence.

Here, fire emission uncertainties had a significant influence on plume transport and downwind $PM_{2.5}$ concentration predictions. Future studies should investigate whether downwind smoke predictions, with Daysmoke or other models, for various burns are subject to similar levels of uncertainty due to emission uncertainties. While existing fire and plume transport models are useful for predicting smoke effects downwind, practitioners of prescribed burning should make firing decisions considering the magnitude of uncertainties associated with concentration predictions due to various sources of uncertainty in emissions.

Acknowledgements

This study was made possible with support from the Joint Fire Science Program (JFSP 081604 and JFSP 081606), the Strategic Environmental Research and Development Program (SERDP RC-1647) and NASA Air Quality Applied Science Team (NNX11AI55G). This publication was made possible also by the US EPA Science to Achieve Results Program (RD83521701). Its contents are solely the responsibility of the grantee and do not necessarily represent the official views of the US EPA. Further, US EPA does not endorse the purchase of any commercial products or services mentioned in the publication. Special thanks are due to those who participated in Rx-CADRE at Eglin AFB and helped gathering burn information and data, especially Brett Williams from Jackson Guard, Eglin AFB Fire Management, and Boris Galvis and Fernando Garcia-Menendez from Georgia Institute of Technology. We also acknowledge David Combs and Ken Forbus from USDA Forest Service for conduction ceilometer measurements, as well as Chris Pressley, Bill Mitchell and Bill Squier of EPA and Rob Gribble of ISSI Inc. for conducting aerostat measurements.

References

Achtemeier GL (2008) Effects of moisture released during forest burning on fog formation and implications for visibility. *Journal of Applied Meteorology and Climatology* **47**(5), 1287–1296. doi:10.1175/2007JAMC1721.1

Achtemeier G, Goodrick S, Liu Y, Garcia-Menendez F, Hu Y, Odman M (2011) Modeling smoke plume-rise and dispersion from southern United States prescribed burns with daysmoke. *Atmosphere (Toronto)* **2**(3), 358–388. doi:10.3390/ATMOS2030358

Achtemeier G, Goodrick S, Liu Y (2012) Modeling multiple-core updraft plume rise for an aerial ignition prescribed burn by coupling Daysmoke with a cellular automata fire model. *Atmosphere (Toronto)* **3**(3), 352–376. doi:10.3390/ATMOS3030352

Anderson G, Sandberg D, Norheim R (2004) Fire Emission Production Simulator (FEPS) User's Guide. Version 1.0. Available at http://www.fs.fed.us/pnw/fera/feps/FEPS_users_guide.pdf [Verified 25 November 2014]

Andrews PL, Bevins CD, Seli RC (2003) BehavePlus fire modelling system, version 2.0: User's Guide. USDA Forest Service, Rocky Mountain Research Station, General Technical Report RMRS-GTR-106WWW. (Ogden, UT)

Aurell J, Gullett BK (2013) Emission factors from aerial and ground measurements of field and laboratory forest burns in the southeastern US: $PM_{2.5}$, black and brown carbon, VOC, and PCDD/PCDF. *Environmental Science & Technology* **47**(15), 8443–8452.

Boylan JW, Russell AG (2006) PM and light extinction model performance metrics, goals, and criteria for three-dimensional air quality models. *Atmospheric Environment* **40**(26), 4946–4959. doi:10.1016/J.ATMOSENV.2005.09.087

Brown JK (1974). Handbook for inventorying downed woody material. USDA Forest Service, Intermountain Forest and Range Experiment Station, Gen. Tech. Rep. INT-16, (Ogden, UT)

Fernandes PM, Davies GM, Ascoli D, Fernández C, Moreira F, Rigolot E, Stoof CR, Vega JA, Molina D (2013) Prescribed burning in southern Europe: developing fire management in a dynamic landscape. *Frontiers in Ecology and the Environment* **11**(s1), e4–e14. doi:10.1890/120298

French N, Goovaerts P, Kasischke E (2004) Uncertainty in estimating carbon emissions from boreal forest fires. *Journal of Geophysical Research, D, Atmospheres* **109**, D14S08. doi:10.1029/2003JD003635

Garcia-Menendez F, Hu Y, Odman MT (2013) Simulating smoke transport from wildland fires with a regional-scale air quality model: sensitivity to uncertain wind fields. *Journal of Geophysical Research, D, Atmospheres* **118**(12), 6493–6504. doi:10.1002/JGRD.50524

GoogleEarth7.1 (2013). Eglin Air Force Base, Florida USA 30°38′46.17″N, 86°16′36.03″W, elevation 52M. Available at http://www.google.com/earth/index.html. [Verified 20 December 2013]

Grandesso E, Gullett B, Touati A, Tabor D (2011) Effect of moisture, charge size, and chlorine concentration on pcdd/f emissions from simulated open burning of forest biomass. *Environmental Science & Technology* **45**(9), 3887–3894. doi:10.1021/ES103686T

Holton JR (2004). 'An Introduction to Dynamic Meteorology.' (Elsevier/Academic Press: London)

Hu Y, Odman MT, Chang ME, Jackson W, Lee S, Edgerton ES, Baumann K, Russell AG (2008) Simulation of air quality impacts from prescribed fires on an urban area. *Environmental Science & Technology* **42**(10), 3676–3682. doi:10.1021/ES071703K

Jain R, Vaughan J, Heitkamp K, Ramos C, Claiborn C, Schreuder M, Schaaf M, Lamb B (2007) Development of the ClearSky smoke dispersion forecast system for agricultural field burning in the Pacific Northwest. *Atmospheric Environment* **41**(32), 6745–6761. doi:10.1016/J.ATMOSENV.2007.04.058

Keane RE (2012) Describing wildland surface fuel loading for fire management: a review of approaches, methods and systems. *International Journal of Wildland Fire* **22**, 51–62. doi:10.1071/WF11139

Larkin NK, O'Neill SM, Solomon R, Raffuse S, Strand T, Sullivan DC, Krull C, Rorig M, Peterson J, Ferguson SA (2009) The BlueSky smoke modeling framework. *International Journal of Wildland Fire* **18**(8), 906–920. doi:10.1071/WF07086

Laursen KK, Ferek RJ, Hobbs PV, Rasmussen RA (1992) Emission factors for particles, elemental carbon, and trace gases from the Kuwait oil fires. *Journal of Geophysical Research, D, Atmospheres* **97**(D13), 14491–14497. doi:10.1029/92JD01370

Liu Y, Goodrick S, Achtemeier G, Jackson WA, Qu JJ, Wang W (2009) Smoke incursions into urban areas: simulation of a Georgia prescribed burn. *International Journal of Wildland Fire* **18**(3), 336–348. doi:10.1071/WF08082

Liu Y, Goodrick S, Achtemeier G, Forbus K, Combs D (2013) Smoke plume height measurement of prescribed burns in the south-eastern United States. *International Journal of Wildland Fire* **22**(2), 130–147. doi:10.1071/WF11072

Mercer G, Weber R (2001) Fire plumes. In 'Fire Plumes.' (Eds EA Johnson, K Miyanishi) pp. 229–251. (Academic Press: San Diego)

Montiel C, Kraus DT (2010). 'Best Practices of Fire Use: Prescribed Burning and Suppression: Fire Programmes in Selected Case-study Regions in Europe.' (European Forest Institute: Joensuu, Finland)

Ottmar RD (2014) Wildland fire emissions, carbon, and climate: modeling fuel consumption. *Forest Ecology and Management* **317**, 41–50. doi:10.1016/J.FORECO.2013.06.010

Ottmar R, Vihnanek R, Mathey J (2003) Stereo photo series for quantifying natural fuels. Volume VIa: sand hill, sand pine scrub, and hardwood with white pine types in the Southeast United States with supplemental sites for Volume VI. (Ed. ID Boise) National Wildfire Coordinating Group, National Interagency Fire Center, Report PMS 838, p. 78.

Prichard S, Ottmar R, Anderson G (2007). Consume 3.0 user's guide and scientific documentation. USDA Forest Service. Pacific Wildland Fire Sciences Laboratory (Seattle, WA). Available at http://www.fs.fed.us/pnw/fera/research/smoke/consume/consume30_users_guide.pdf [Verified 25 November 2014]

Reid J, Koppmann R, Eck T, Eleuterio D (2005) A review of biomass burning emissions part II: intensive physical properties of biomass burning particles. *Atmospheric Chemistry and Physics* **5**(3), 799–825. doi:10.5194/ACP-5-799-2005

Seiler W, Crutzen P (1980) Estimates of gross and net fluxes of carbon between the biosphere and the atmosphere from biomass burning. *Climatic Change* **2**(3), 207–247. doi:10.1007/BF00137988

Skamarock WC, Klemp JB (2008) A time-split nonhydrostatic atmospheric model for weather research and forecasting applications. *Journal of Computational Physics* **227**(7), 3465–3485. doi:10.1016/J.JCP.2007.01.037

Skamarock J, Klemp W, Dudhia J, Gill D, Barker D, Duda M, Huang X, Wang W, Powers J (2008) A description of the advanced research WRF version 3, NCAR technical note. (NCAR/TN–475+ STR) Available at http://www2.mmm.ucar.edu/wrf/users/docs/arw_v2.pdf [Verified 25 November 2014]

Tian D, Hu Y, Wang Y, Boylan JW, Zheng M, Russell AG (2009) Assessment of biomass burning emissions and their impacts on urban and regional PM2. 5: a Georgia case study. *Environmental Science & Technology* **43**(2), 299–305. doi:10.1021/ES801827S

Urbanski SP, Hao WM, Baker S (2008) Chemical composition of wildland fire emissions. *Developments in Environmental Science* **8**, 79–107. doi:10.1016/S1474-8177(08)00004-1

Urbanski S, Hao W, Nordgren B (2011) The wildland fire emission inventory: western United States emission estimates and an evaluation of uncertainty. *Atmospheric Chemistry and Physics* **11**(24), 12973–13000. doi:10.5194/ACP-11-12973-2011

US EPA (1995) Compilation of Air Pollutant Emission Factors, AP-42, 5th edn, Vol. 1: Stationary Point and Area Sources. (US EPA: Research Triangle Park, NC)

US EPA (2013). The 2011 National Emissions Inventory. Available at http://www.epa.gov/ttn/chief/net/2011inventory.html [Verified 25 November 2014]

Weise DR, Wright CS (2014) Wildland fire emissions, carbon and climate: characterizing wildland fuels. *Forest Ecology and Management* **317**, 26–40. doi:10.1016/J.FORECO.2013.02.037

Wiedinmyer C, Quayle B, Geron C, Belote A, McKenzie D, Zhang XY, O'Neill S, Wynne KK (2006) Estimating emissions from fires in North America for air quality modeling. *Atmospheric Environment* **40**(19), 3419–3432. doi:10.1016/J.ATMOSENV.2006.02.010

Wilson J, Sawford B (1996) Review of Lagrangian stochastic models for trajectories in the turbulent atmosphere. *Boundary-Layer Meteorology* **78**(1–2), 191–210. doi:10.1007/BF00122492